Available online at www.sciencedirect.com
ScienceDirect
Journal of Magnetic Resonance 184 (2007) 330–336
JMR Journal of Magnetic Resonance
www.elsevier.com/locate/jmr

Communication

2D separated-local-field spectra from projections of 1D experiments

Kresten Bertelsen, Jan M. Pedersen, Niels Chr. Nielsen, Thomas Vosegaard *

Center for Insoluble Protein Structures (inSPIN), Interdisciplinary Nanoscience Center (iNANO) and Department of Chemistry, University of Aarhus, DK-8000 Aarhus C, Denmark

Received 20 July 2006; revised 2 October 2006
Available online 2 November 2006

Abstract

A novel procedure for reconstruction of 2D separated-local-field (SLF) NMR spectra from projections of 1D NMR data is presented. The technique, dubbed SLF projection reconstruction from one-dimensional spectra (SLF-PRODI), is particularly useful for uniaxially oriented membrane protein samples and represents a fast and robust alternative to the popular PISEMA experiment which correlates ^{1}H–^{15}N dipole–dipole couplings with ^{15}N chemical shifts. The different 1D projections in the SLF-PRODI experiment are obtained from 1D spectra recorded under influence of homonuclear decoupling sequences with different scaling factors for the heteronuclear dipolar couplings. We demonstrate experimentally and numerically that as few as 2–4 1D projections will normally be sufficient to reconstruct a 2D SLF-PRODI spectrum with a quality resembling typical PISEMA spectra, leading to significant reduction of the acquisition time.

Keywords: PISEMA; Projection–reconstruction; Separated-local-field; Oriented bilayer samples; SLF-PRODI; Radial sampling

1. Introduction

Multidimensional NMR experiments have played a key role in driving the field of NMR spectroscopy forward since the concept was introduced in the early seventies [1,2]. 2D, 3D, and even 4D experiments are now routinely used in the experimental toolbox for, e.g., protein structure determination, where the large number of resonances requires high-dimensional NMR experiments to resolve all peaks and/or to provide the desired internuclear correlations. The major drawback of multidimensional NMR spectroscopy is that the experimental time increases dramatically with the number of indirect dimensions. In this time not only the sample has to be stable but also the performance of the RF field irradiation, which may be an issue of concern in biological solid-state NMR spectroscopy using relatively strong RF field strengths on heterogeneous samples [3,4].

To partly alleviate such problems, multidimensional experiments with reduced dimensionality have been developed in order to reduce the acquisition time [5–18]. One of these is the projection–reconstruction (PR) technique [16] in which the multidimensional spectrum is reconstructed from the projections of a number of lower-dimensional spectra. The experimental setup for PR experiments relies on acquiring multidimensional experiments with simultaneous incrementation in two or more indirect dimensions. The direction of the projection is controlled by the ratio between the simultaneous time increments. In the case of simple spectra with few resonances, only a small number of projections is needed, while in the case of dense spectra, a more systematic PR approach like radial sampling is preferable [17,18] potentially in combination with advanced data processing [19]. Reduced-dimensionality techniques have been successfully applied for a number of correlation experiments in liquid- [5–7,9–18] and solid-state [8] NMR spectroscopy.

The study of peptides and proteins in oriented phospholipid bilayers by solid-state NMR spectroscopy is a promising route to membrane protein structure determination

* Corresponding author. Fax: +45 8619 6199.
E-mail address: tv@chem.au.dk (T. Vosegaard).

1090-7807/$ - see front matter © 2006 Elsevier Inc. All rights reserved.
doi:10.1016/j.jmr.2006.10.005

[20–29]. A key experiment for such studies is a 2D separated-local-field (SLF) experiment [30] which correlates the protein backbone amide ^{1}H–^{15}N dipolar coupling with the ^{15}N chemical shift, since it provides important structural constraints and offers a high spectral resolution [31]. Fig. 1 displays some commonly used SLF pulse sequences. The simplest SLF experiment with ^{1}H homonuclear decoupling during t_1 employs the pulse sequence in Fig. 1c for the encoding of the indirect dimension and uses a π pulse on the ^{15}N channel to refocus the ^{15}N chemical shift. For oriented protein samples, the most popular variants of the SLF experiment are the polarization-inversion spin-exchange at the magic angle (PISEMA) experiment [32] (Fig. 1d) and the more recent magic-sandwich-based [33] experiment dubbed SAMMY [34] (Fig. 1e). As seen in Fig. 1 these experiments consist of a cross-polarization (CP) block to transfer magnetization from ^{1}H to ^{15}N, followed by the t_1 evolution period which for the PISEMA experiment is a spin-exchange at the magic angle (SEMA) block which decouples homonuclear ^{1}H–^{1}H dipole–dipole couplings and suppresses ^{15}N chemical shift evolution, leaving only the desired heteronuclear ^{1}H–^{15}N dipole–dipole couplings active. In the SAMMY experiment the SEMA block is replaced by a magic-sandwich sequence [33] on the ^{1}H channel accompanied by a phase-alternating spin lock on the ^{15}N channel. Because of the high resolution in the indirect dimension the t_1 period may need to be as long as 5–10 ms [35]. The ^{1}H–^{15}N dipole–dipole coupling couplings restrict the indirect spectral width to be ~25 kHz inducing the need for several hundreds of t_1 increments to achieve maximum resolution thus leading to very long experiment times, although a faster variant employing reduced data sampling and maximum entropy reconstruction has recently been proposed [36].

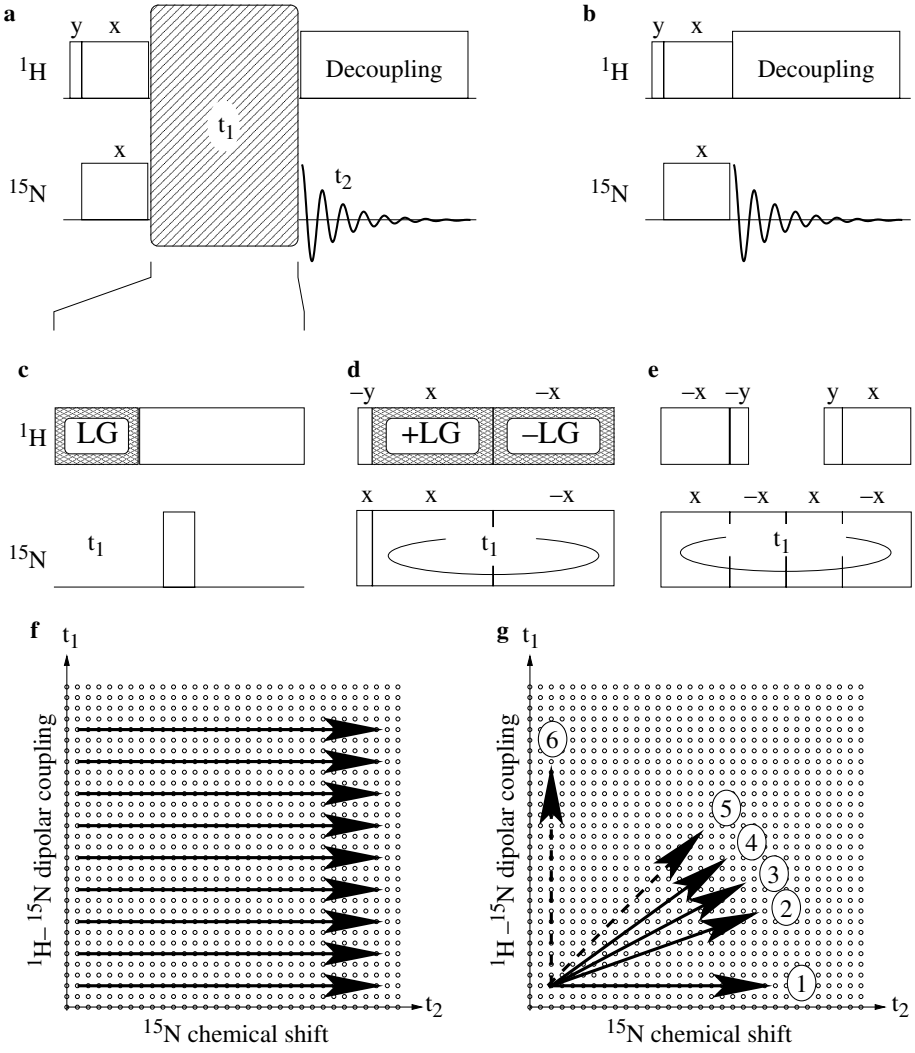

Fig. 1. Schematic illustration of the SLF-PRODI principle. (a) Generic SLF and (b) CP pulse sequences used in this work. The indirect evolution period of the SLF experiment may use different pulse schemes of which this figure reports (c) standard SLF, (d) PISEMA, and (e) SAMMY variants. The acquisition of the 2D time-domain matrices is illustrated in (f) for SLF experiments and (g) SLF-PRODI employing the CP pulse sequence with the following decoupling schemes: SPINAL-64 (1), MSHOT-3 (2), MREV-8 (3), and FSLG (4) decoupling, and no decoupling (5). The vertical arrow (6) can only be achieved using pulsed chemical shift suppression (e.g., SEMA) on the ^{15}N channel.

In this Communication, we present a fast and experimentally robust alternative to the two-dimensional SLF pulse sequences based on reconstruction of the SLF spectrum from one-dimensional experiments. We call this experiment SLF projection reconstruction of one-dimensional spectra (SLF-PRODI).

2. Results and discussion

The idea of SLF-PRODI is illustrated in Fig. 1 and uses the standard cross-polarization (CP) pulse sequence shown in Fig. 1b with different decoupling schemes during acquisition. In a standard 2D SLF experiment where the indirect t_1 dimension encodes the ^{1}H–^{15}N dipole–dipole coupling while the direct t_2 dimension acquires the ^{15}N chemical shift, the acquisition of the 2D time-domain matrix follows the arrows shown in Fig. 1f using stepwise increments for t_1 between each t_2 slice. With SLF-PRODI we exploit the fact that applying homonuclear ^{1}H decoupling during the acquisition period of the CP experiment will not remove the heteronuclear coupling but only scale it down by the so-called scaling factor of the decoupling sequence. This implies that such an experiment will sample both the ^{1}H–^{15}N dipole–dipole coupling and ^{15}N chemical shift. Fig. 1g shows that this corresponds to simultaneous t_1 and t_2 increments in the 2D time-domain matrix resulting in projections with different angles with respect to the t_1 and t_2 axes. The angle of a particular experiment is determined by the scaling factor of the homonuclear decoupling sequence. For illustration, Fig. 1g reports the acquisition traces of regular proton decoupling, the magic-sandwich based sequence MSHOT-3 [37], MREV-8 [38,39], FSLG [40], no decoupling, and SEMA. These sequences display ^{1}H–^{15}N dipole–dipole (S_{DD})/^{15}N chemical shift (S_{CS}) scaling factors of 0.35/1 (MSHOT-3), 0.47/1 (MREV-8), 0.58/1 (FSLG), 1/1 (no decoupling), and 0.82/0 (SEMA). In the 2D time-domain matrix representation in Fig. 1g experiments employing one of these sequences will follow a trajectory along an axis with a slope defined by the scaling factors, i.e., with an angle of arctan(S_{DD}/S_{CS}) relative to the ^{15}N chemical shift axis. We note that angles larger than 45° can not be achieved using the pulse sequence in Fig. 1b but need pulses on ^{15}N to scale down the chemical shift [41], e.g., by the SEMA sequence.

Experimental SLF-PRODI spectra for a ^{15}N-labeled *N*-acetyl leucine (NAL) crystal are shown in Fig. 2a and result from regular proton decoupling using the SPINAL-64 [42] sequence (left), FSLG (center), and MSHOT-3 (right) decoupling. For illustration Fig. 2b shows the 2D representation of these spectra, each of which consists of two projections mirrored vertically. The reason for having two projections from each experiment is that the dipolar dimension contains symmetric doublets reflecting that the pulse sequences are insensitive to the sign of the heteronuclear dipole–dipole coupling. The slopes of the projections are defined by the ^{1}H–^{15}N dipole–dipole and ^{15}N chemical shift scaling factors as discussed above. The final SLF-PRODI reconstruction should only show peaks where all projections have intensity. Numerically, this is done by comparing all available projections and assigning the minimum intensity found in these projections to the reconstructed spectrum. The SLF-PRODI spectrum resulting from reconstruction of the SPINAL-64 and FSLG projections (referred to as a SLF-PRODI-2$_{SPINAL,FSLG}$ spectrum since it results from these two projections) is shown in Fig. 2c along with a conventional PISEMA spectrum in Fig. 2d. These spectra have comparable resolution in the two dimensions. For the NAL crystal, we observe linewidths of ~50 Hz using SPINAL-64 decoupling and in favorable cases down to 100 Hz with FSLG decoupling. In the reconstructed 2D SLF-PRODI spectrum the resulting ^{1}H–^{15}N dipolar linewidths are somewhat larger (typically around 300 Hz) because of the modest scaling factor of the FSLG sequence. However, despite this fact the SLF-PRODI linewidths compare reasonably well with state-of-the-art achievements (~200 Hz) using the PISEMA or SAMMY pulse sequences, especially when considering that the present PISEMA spectrum has been recorded using 128 t_1 increments while the SLF-PRODI spectrum was obtained from only two 1D projections. The PISEMA experiment employed 8 scans for each t_1 increment corresponding to a total of 1024 scans, while for the SLF-PRODI spectrum, the SPINAL-64 experiment employed 8 scans and the FSLG spectrum employed 64 scans to compensate for the lower peak intensity resulting from the doublet splitting of all lines. Thus, only a total of 72 scans was needed for the SLF-PRODI-2 spectrum, which corresponds to a 14-fold reduction of the experiment time. We note that in the present example, the SLF-PRODI-3$_{SPINAL,FSLG,MSHOT}$ (not shown) does not improve the resolution compared to the SLF-PRODI-2 spectrum in Fig. 2c. This may be ascribed to the fact that the MSHOT-3 sequence, although theoretically better, in the present case led to spectra with larger absolute linewidths than the FSLG and SPINAL experiments. Similar behavior was observed by Wu et al. in the original PISEMA work [32], where various decoupling sequences were compared. It is important to emphasize, however, that the primary aim of the SLF-PRODI-3 experiment is not to improve the resolution of SLF-PRODI-2 but to reduce the number of artifacts being particularly important for multiple-labeled samples (*vide infra*).

To investigate the ability of SLF-PRODI to reconstruct the correct 2D spectrum Figs. 3 and 4 show sets of SIMPSON/SIMMOL simulations [43–45] designed to challenge the performance of the technique for cases with different number of resonances in the spectra (e.g., different isotope labeling patterns). Fig. 3a–c show simulated SLF-PRODI spectra for three ^{1}H–^{15}N spin pairs, which could represent three individual ^{15}N labeled amino acids in a peptide, employing SLF-PRODI-2 and SLF-PRODI-3 reconstructions. For comparison, Fig. 3d shows the corresponding PISEMA spectrum. In this example we observe that the two SLF-PRODI-2 spectra in Fig. 3a (SLF-PRODI-2$_{SPI-}$

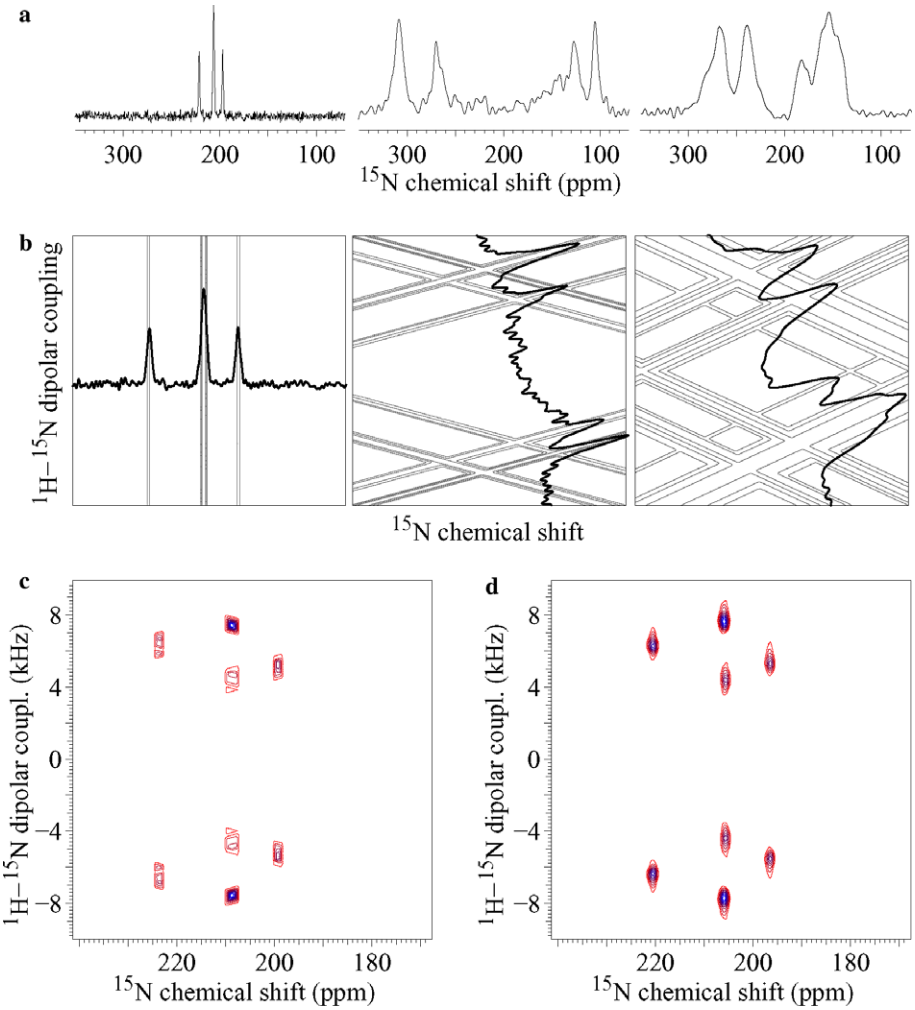

Fig. 2. Experimental SLF-PRODI (a–c) and PISEMA (d) spectra. The three panels in (a) display the spectra obtained using SPINAL-64 (left), FSLG (center), and MSHOT-3 (right) decoupling for a single crystal of ^{15}N labeled *N*-acetyl leucine along with the corresponding 2D projections in (b). The reconstructed 2D SLF-PRODI-2$_{\mathrm{SPINAL,FSLG}}$ and PISEMA spectra are shown in (c) and (d), respectively.

$_{\mathrm{NAL,FSLG}}$) and 3b (SLF-PRODI-2$_{\mathrm{SPINAL,MSHOT}}$) fail to eliminate the artificial peaks indicated by arrows. Only when employing the three projections all together as shown in Fig. 3c (SLF-PRODI-3$_{\mathrm{SPINAL,FSLG,MSHOT}}$) the reconstructed spectrum is free from artifacts and provides the correct reconstruction.

In a more challenging case, Fig. 4 numerically explores the possibility to reconstruct the spectrum of a uniformly ^{15}N-labeled α-helix peptide. Using typical parameters for the nuclear spin interactions [43] for an ideal 18-residue α-helix (torsion angles of $\phi = -65°$ and $\psi = -40°$) with a tilt of 30° relative to the magnetic field, the characteristic PISA wheel resonance pattern [46,47] appears in the simulated PISEMA spectrum (Fig. 4f). We observe that the SLF-PRODI-2$_{\mathrm{SPINAL,FSLG}}$ reconstruction (Fig. 4a) displays vast amounts of artificial peaks, while the PISA wheel appears clearly in the SLF-PRODI-3$_{\mathrm{SPINAL,FSLG,MSHOT}}$ (Fig. 4b) and SLF-PRODI-4$_{\mathrm{SPINAL,FSLG,MSHOT,MREV}}$ (Fig. 4c) reconstructions. However, even the SLF-PRODI-4 reconstruction still contains some artificial peaks, and while the recognition of the PISA wheel will be sufficient to obtain information about the helix tilt, the remaining artifacts may be problematic for the assignment and detailed interpretation of the spectrum. To improve this, we would need a combination of more experiments resulting from homonuclear decoupling sequences with different scaling factors, as suggested by the simulations in Fig. 4d and e. Fig. 4d shows a SLF-PRODI-4 spectrum resulting from 1D experiments with heteronuclear dipolar scaling factors of 0, 0.33, 0.67, and 1, which is free from the above artifacts. While it is not likely to find a homonuclear decoupling sequence with a heteronuclear dipolar scaling factor of 1, Fig. 4e shows a SLF-PRODI-5 spectrum from experiments with scaling factors of 0, 0.2, 0.4, 0.6, and 0.8, which also removes all artificial peaks.

Based on experimental and numerical results we judge that SLF-PRODI-2 or SLF-PRODI-3 experiments should be sufficient to obtain reliable 2D spectra for sparsely labeled samples, while a uniformly labeled peptide may be at the limit of the capability of SLF-PRODI with the present set of homonuclear decoupling sequences. However, it is easily foreseen that experiments employing homonuclear

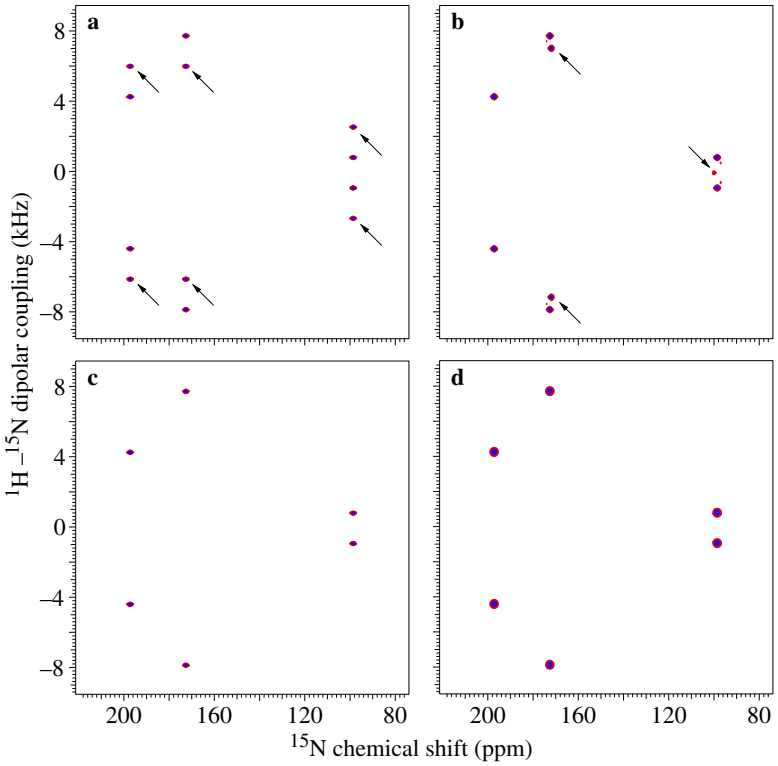

Fig. 3. Simulated 9.4-T SLF-PRODI and PISEMA spectra for a sample with three ^{1}H–^{15}N spin pairs. The spectra show reconstructions from (a) SLF-PRODI-2$_{\text{SPINAL,FSLG}}$, (b) SLF-PRODI-2$_{\text{SPINAL,MSHOT}}$, (c) SLF-PRODI-3$_{\text{SPINAL,FSLG,MSHOT}}$ along with a PISEMA spectrum (d). Chemical shifts of 100, 175, and 200 ppm and dipolar couplings of 0.9, 7.8, and 4.3 kHz were assumed.

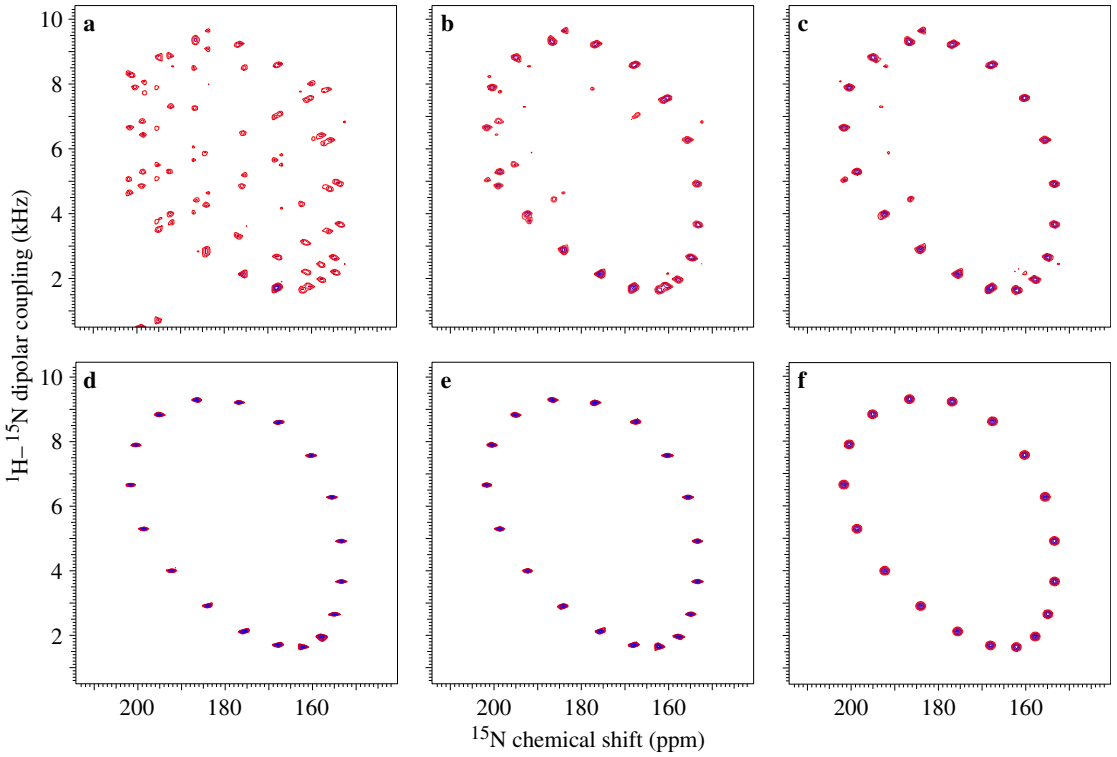

Fig. 4. Simulated 9.4-T SLF-PRODI and PISEMA spectra for an ideal uniformly ^{15}N labeled α-helix with 18 residues. The spectra show reconstructions from (a) SLF-PRODI-2$_{\text{SPINAL,FSLG}}$, (b) SLF-PRODI-3$_{\text{SPINAL,FSLG,MSHOT}}$, (c) SLF-PRODI-4$_{\text{SPINAL,FSLG,MSHOT,MREV}}$, (d) SLF-PRODI-4 from experiments with heteronuclear dipolar scaling factors of 0, 0.33, 0.67, and 1, (e) SLF-PRODI-5 from experiments with heteronuclear dipolar scaling factors of 0, 0.2, 0.4, 0.6, and 0.8, along with a PISEMA spectrum (f).

decoupling sequences with adjustable scaling factors may be used to sample the 2D time domain in a more systematic way (i.e., in a fashion similar to radial sampling [17,18]) so this limitation can be overcome. Such experiments could for example take inspiration from the concept of time-averaged nutation [48] which changes the scaling factor of the CP experiment. One could envisage experimental realization of different scaling by evolution under mixing decoupling sequences with different scaling factors.

In the practical realization of the SLF-PRODI experiments, we will always start with the vertical SPINAL-64 decoupling projection followed by FSLG since this decoupling sequence has an appreciably large scaling factor. Only if the reconstructed 2D spectrum contains artificial peaks will we continue with acquisition of other projections.

3. Conclusions

In conclusion, we have presented the SLF-PRODI technique which allows us to reconstruct two-dimensional separated-local-field spectra from few 1D projections. The technique is particularly useful for sparsely labeled samples, e.g., with residue-specific ^{15}N labeling, and allows for very fast acquisition of 2D spectra for such samples. In our practical example a time-saving of an order of magnitude was reported. For more densely labeled samples SLF-PRODI may prove to be very valuable for reduction of the dimensionality of higher-dimensional double- and triple-resonance experiments, and we anticipate that four- and even five-dimensional spectra may be acquired within a reasonable time-frame. Further work along these lines is in progress.

4. Experimental

All experiments were performed on a Bruker Avance 400 spectrometer with a 9.4 T magnet employing a 4 mm Bruker triple-resonance MAS probe in double-resonance configuration. The ^{1}H RF field strength was 100 kHz for the 90° pulse and decoupling period for all experiments, while it was reduced to 41.8 kHz during the 1 ms CP period as well as the t_1 period of the PISEMA experiment. The ^{15}N RF field strength was 41.8 kHz during CP and 50 kHz during t_1 of the PISEMA experiment. The 1D SPINAL-64 was acquired using 8 scans while the homonuclear decoupling experiments employed 64 scans. The PISEMA experiment employed 128 t_1 increments, each acquired using 8 scans.

Reconstruction of the 2D spectra was performed either on the spectrometer employing Bruker AU programs which will be available for download from our web site (http://www.bionmr.chem.au.dk), or using SIMPSON.

The ^{15}N labeled *N*-acetyl leucine (NAL) crystal was synthesized by suspending ^{15}N L-leucine (0.50 g, 3.78 mmole) and acetic anhydride (0.46 g, 4.54 mmole) in glacial acetic acid (10 cm^3) followed by stirring overnight (or until homogeneity is achieved) at room temperature. The resulting mixture was evaporated to dryness under reduced pressure, acetone (15 cm^3, HPLC grade) was added and the suspension was filtered to afford a filtrate which was evaporated under reduced pressure to afford ^{15}N NAL as a colorless solid. The solid was dissolved in a minimal amount of boiling methanol and left to cool whilst allowing for slow evaporation of methanol (perforated parafilm lid) overnight. This procedure was repeated twice to form sufficiently large crystals.

Acknowledgments

Support from the Danish National Research Foundation, the Danish Natural Science Research Council, and the Danish Biotechnology Instrument Centre (DABIC) is acknowledged.

References

[1] J. Jeener. (September 1971), International Ampere Summer School, Basko Polje, Yugoslavia; lecture notes published (1994) in NMR and More in Honour of A. Abragam, eds. Goldman, M.; Porneuf, M. (Les Editions de Physique, Les Ulis, France).
[2] R.R. Ernst, G. Bodenhausen, A. Wokaun, Principles of Nuclear Magnetic Resonance in One and Two Dimensions, Clarendon Press, Oxford, 1987.
[3] J.A. Stringer, C.E. Bronnimann, C.G. Mullen, D.H. Zhou, S.A. Stellfox, Y. Li, E.H. Williams, C.M. Rienstra, Reduction of RF-induced sample heating with a scroll coil resonator structure for solid-state NMR probes, J. Magn. Reson. 173 (2005) 40–48.
[4] P.L. Gor'kov, E.Y. Chekmenev, R. Fu, J. Hu, T.A. Cross, M. Cotton, W.H. Brey, A large volume flat coil probe for oriented membrane proteins, J. Magn. Reson. 181 (2006) 9–20.
[5] T. Szyperski, G. Wider, J.H. Bushweller, K. Wüthrich, Reduced dimensionality in triple-resonance NMR experiments, J. Am. Chem. Soc. 115 (1993) 9307–9308.
[6] J.-P. Simorre, B. Brutscher, M.S. Caffrey, D. Marion, Assignment of NMR spectra of proteins using triple-resonance two-dimensional experiments, J. Biomol. NMR 4 (1994) 325–333.
[7] N.M. Loening, J. Keeler, G.A. Morris, One-dimensional DOSY, J. Magn. Reson. 153 (2001) 103–112.
[8] N.S. Astrof, C.E. Lyon, R.G. Griffin, Triple resonance solid state NMR experiments with reduced dimensionality evolution periods, J. Magn. Reson. 152 (2001) 303–307.
[9] T. Szyperski, D.C. Yeh, D.K. Sukumaran, N.H.B. Moseley, G.T. Montelione, Reduced-dimensionality NMR spectroscopy for high-throughput protein resonance assignment, Proc. Natl. Acad. Sci. USA 99 (2002) 8009–8014.
[10] L. Frydman, T. Scherf, A. Lupulescu, The acquisition of multidimensional NMR spectra within a single scan, Proc. Natl. Acad. Sci. USA 99 (2002) 15858–15862.
[11] Ē. Kupče, R. Freeman, Two-dimensional Hadamard spectroscopy, J. Magn. Reson. 162 (2003) 300–310.
[12] W. Koźmiński, I. Zhukov, Multiple quadrature detection in reduced dimensionality experiments, J. Biomol. NMR 26 (2003) 157–166.
[13] P. Pelupessy, Adiabatic single scan two-dimensional NMR spectroscopy, J. Am. Chem. Soc. 125 (2003) 12345–12350.
[14] S. Kim, T. Szyperski, GFT NMR, a new approach to rapidly obtain precise high-dimensional NMR spectral information, J. Am. Chem. Soc. 125 (2003) 1385–1393.
[15] R. Brüschweiler, F. Zhang, Covariance nuclear magnetic resonance spectroscopy, J. Chem. Phys. 120 (2004) 5253–5260.
[16] Ē. Kupče, R. Freeman, Projection-reconstruction technique for speeding up multidimensional NMR spectroscopy, J. Am. Chem. Soc. 126 (2004) 6429–6440.

[17] Ē Kupče, R. Freeman, The radon transform: a new scheme for fast multidimensional NMR, Concepts Magn. Reson. 22A (2004) 4–11.
[18] Ē. Kupče, R. Freeman, Fast multidimensional NMR: radial sampling of evolution space, J. Magn. Reson. 173 (2005) 317–321.
[19] K. Kazimierczuk, W. Koźmiński, I. Zhukov, Two-dimensional Fourier transform of arbitrarily sampled NMR data sets, J. Magn. Reson. 179 (2006) 323–328.
[20] R.R. Ketchem, K.-C. Lee, S. Huo, T.A. Cross, Macromolecular structural elucidation with solid-state NMR-derived orientational constraints, J. Biomol. NMR 8 (1996) 1–14.
[21] S.J. Opella, F.M. Marassi, J.J. Gesell, A.P. Valente, Y. Kim, M. Oblatt-Montal, M. Montal, Structures of the M2 channel-lining segments from nicotinic acetylcholine and NMDA receptors by NMR spectroscopy, Nat. Struct. Biol. 6 (1999) 374–379.
[22] K.G. Valentine, S.F. Liu, F.M. Marassi, G. Veglia, S.J. Opella, F.X. Ding, S.H. Wang, B. Arshava, J.M. Becker, F. Naider, Structure and topology of a peptide segment of the 6th transmembrane domain of the *Saccharomyces cerevisae* α-factor receptor in phospholipid bilayers, Biopolymers 59 (2001) 243–256.
[23] K. Nishimura, S. Kim, L. Zhang, T.A. Cross, The closed state of a H^+ channel helical bundle combining precise orientational and distance restraints from solid state NMR, Biochemistry 41 (2002) 13170–13177.
[24] F.M. Marassi, S.J. Opella, Simultaneous assignment and structure determination of a membrane protein from NMR orientational restraints, Protein Sci. 12 (2003) 403–411.
[25] A.C. Zeri, M.F. Mesleh, A.A. Nevzorov, S.J. Opella, Structure of the coat protein in fd filamentous bacteriophage particles determined by solid-state NMR spectroscopy, Proc. Natl. Acad. Sci. USA 100 (2003) 6458–6463.
[26] S.H. Park, A.A. Mrse, A.A. Nevzorov, M.F. Mesleh, M. Oblatt-Montal, M. Montal, S.J. Opella, Three-dimensional structure of the channel-forming trans-membrane domain of virus protein "u" (Vpu) from HIV-1, J. Mol. Biol. 333 (2003) 409–424.
[27] D.S. Thiriot, A.A. Nevzorov, L. Zagyanskiy, C.H. Wu, S.J. Opella, Structure of the coat protein Pf1 bacteriophage determined by solid-state NMR spectroscopy, J. Mol. Biol. 341 (2004) 869–879.
[28] D.S. Thiriot, A.A. Nevzorov, S.J. Opella, Structural basis of the temperature transition of Pf1 bacteriophage, Protein Sci. 14 (2005) 1064–1070.
[29] S.H. Park, S. Prytulla, A.A. de Angelis, J.M. Brown, H. Kiefer, S.J. Opella, High-resolution NMR spectroscopy of a GPCR in aligned bicelles, J. Am. Chem. Soc. 128 (2006) 7402–7403.
[30] R.K. Hester, J.L. Ackerman, B.L. Neff, J.S. Waugh, Separated local field spectra in NMR: determination of structure of solids, Phys. Rev. Lett. 36 (1976) 1081–1083.
[31] T. Vosegaard, N.C. Nielsen, Towards high-resolution solid-state NMR on large uniformly ^{15}N- and [^{13}C,^{15}N]-labeled membrane proteins in oriented lipid bilayers, J. Biomol. NMR 22 (2002) 225–247.
[32] C.H. Wu, A. Ramamoorthy, S.J. Opella, High-resolution heteronuclear dipolar solid-state NMR spectroscopy, J. Magn. Reson. 109 (1994) 227–231.
[33] W.-K. Rhim, A. Pines, J.S. Waugh, Time-reversal experiments in dipolar-coupled spin systems, Phys. Rev. B 3 (1971) 684–696.
[34] A.A. Nevzorov, S.J. Opella, A "magic sandwich" pulse sequence with reduced offset dependence for high-resolution separated local field spectroscopy, J. Magn. Reson. 164 (2003) 182–186.
[35] A. Ramamoorthy, C.H. Wu, S.J. Opella, Experimental aspects of multidimensional solid-state NMR correlation spectroscopy, J. Magn. Reson. 140 (1999) 131–140.
[36] D.H. Jones, S.J. Opella, Application of maximum entropy reconstruction to PISEMA spectra, J. Magn. Reson. 179 (2006) 105–113.
[37] M. Hohwy, N.C. Nielsen, Elimination of high order terms in multiple pulse nuclear magnetic resonance spectroscopy: application to homonuclear decoupling in solids, J. Chem. Phys. 106 (1997) 7571–7586.
[38] P. Mansfield, Symmetrized pulse sequences in high-resolution NMR in solids, J. Phys. C: Solid State Phys. 4 (1971) 1444–1452.
[39] W.-K. Rhim, D.D. Elleman, R.W. Vaughan, Analysis of multiple pulse NMR in solids, J. Chem. Phys. 59 (1973) 3740–3749.
[40] A. Bielecki, A.C. Kolbert, H.J.M. de Groot, R.G. Griffin, M.H. Levitt, Frequency-switched Lee–Goldburg sequences in solids, Adv. Magn. Reson. 14 (1990) 111–124.
[41] W.P. Aue, D.J. Ruben, R.G. Griffin, Uniform chemical shift scaling in rotating solids, J. Magn. Reson. 46 (1982) 354–357.
[42] N. Shiha, C.V. Grant, C.H. Wu, A.A. de Angelis, S.C. Howell, S.J. Opella, SPINAL modulated decoupling in high field double- and triple-resonance solid-state NMR experiments on stationary samples, J. Magn. Reson. 177 (2005) 197–202.
[43] M. Bak, J.T. Rasmussen, N.C. Nielsen, SIMPSON: a general simulation program for solid-state NMR spectroscopy, J. Magn. Reson. 147 (2000) 296–330, SIMPSON is open-source software freely available from the web site http://www.bionmr.chem.au.dk..
[44] M. Bak, R. Schultz, T. Vosegaard, N.C. Nielsen, Specification and visualization of anisotropic interaction tensors in polypeptides and numerical simulations in biological solid-state NMR, J. Magn. Reson. 154 (2002) 28–45, SIMMOL is open-source software freely available from the web site http://www.bionmr.chem.au.dk..
[45] T. Vosegaard, A. Malmendal, N.C. Nielsen, The flexibility of SIMPSON and SIMMOL for numerical simulations in solid- and liquid-state NMR spectroscopy, Chem. Monthly 133 (2002) 1555–1574.
[46] J. Wang, J. Denny, C. Tian, S. Kim, Y. Mo, F. Kovacs, Z. Song, K. Nishimura, Z. Gan, R. Fu, J.R. Quine, T.A. Cross, Imaging membrane protein helical wheels, J. Magn. Reson. 144 (2000) 162–167.
[47] F.M. Marassi, S.J. Opella, A solid-state NMR index of helical membrane protein structure and topology, J. Magn. Reson. 144 (2000) 150–155.
[48] K. Takegoshi, C.A. McDowell, Cross polarization using a time-averaged precession frequency. A simple technique to reduce radio frequency power requirements for magnetization transfer experiments in solids, J. Magn. Reson. 67 (1986) 356–361.